HOKKAIDO UNIVERSITY

| | |
|---|---|
| Title | Structure and magnetic properties of double perovskites SrCaLnRuO6 (Ln = La, Pr, Nd) |
| Author(s) | Sasaki, Akira; Doi, Yoshihiro; Hinatsu, Yukio |
| Citation | Journal of Alloys and Compounds, 477(1-2), 900-904<br>https://doi.org/10.1016/j.jallcom.2008.11.041 |
| Issue Date | 2009-05-27 |
| Doc URL | https://hdl.handle.net/2115/38693 |
| Type | journal article |
| File Information | 477-1-2_p900-904.pdf |




Hokkaido University Collection of Scholarly and Academic Papers : HUSCAP

# Structure and Magnetic Properties of Double Perovskites SrCa*Ln*$RuO_6$ (*Ln* = La, Pr, Nd)

Akira Sasaki, Yoshihiro Doi and Yukio Hinatsu

Division of Chemistry, Graduate School of Science, Hokkaido University,
Sapporo 060-0810, Japan

e-mail: hinatsu@sci.hokudai.ac.jp
telephone: +81-11-706-2702
fax: +81-11-706-2702

## Abstract

Double perovskite compounds $SrCaLnRuO_6$ (Ln = La, Pr, Nd) were prepared as a single phase. X-ray diffraction measurements show that $Ca^{2+}$ and $Ln^{3+}$ ions are partially disordered at the A site and half of the B site of the perovskite $ABO_3$, and that $Ca^{2+}/Ln^{3+}$ and $Ru^{5+}$ ions are regularly ordered at the B site. These compounds should be represented by $SrCa_{1-x}Ln_x[Ln_{1-x}Ca_x]RuO_6$ and x = 0.83 – 0.93 for Ln = La, Pr, and Nd. Magnetic and specific heat measurements show that any of these compounds orders antiferromagnetically at 10 – 12 K, which is due to the magnetic interactions between $Ru^{5+}$ ions. The analysis of the magnetic entropy change indicates that the ground states of $Ru^{5+}$ and $Ln^{3+}$ ions are both doublet.

## 1. Introduction

The perovskite-type oxides have the general formula $ABO_3$, in which A represents a large metal cation and B represents a small one. The perovskite structure can be described as a framework of corner-shared $BO_6$ octahedra, which contain A cations at 12-coordinate sites. Double perovskite-type oxides have the formula $A_2B'B''O_6$, in which the primes indicate the different ions in different oxidation states, and B' and B'' cations are regularly ordered, i.e., 1:1 arrangement of B' and B'' ions has been observed over the six-coordinate B sites [1]. Since the B cations generally determine the physical properties of perovskites, different kinds of B' and B'' ion should show a variety of the physical properties of double perovskite oxides.

The preparation, crystal structures and magnetic properties of double perovskite oxides containing Ru ion, $A_2LnRuO_6$ (A = alkali-earth metals), where Ln represents a rare earth ion, have been studied [2-14]. The electronic structure of $Ru^{5+}$ is $[Kr]4d^3$ ([Kr]: krypton electronic core), which means that it has the largest spin (S = 3/2). Such highly oxidized cations from the second or third transition series sometimes show quite unusual magnetic behavior. Any of the double perovskites $Ba_2LnRuO_6$ (Ln = La ~ Lu) [2, 4, 5, 9-12] and $Sr_2LnRuO_6$ (Eu ~ Lu) [3, 4, 6-8, 12-14] showed an antiferromagnetic transition at low temperatures, and the transition temperature is higher than that for the compounds in which the magnetic ion at the B site is $Ru^{5+}$ ion only. Among them, the transition temperature for $Ba_2PrRuO_6$ was astonishingly as high as

117 K [10], and $Ba_2NdRuO_6$ transformed to the antiferromagnetic state at 57 K [9].

In the case of $Ca_2LnRuO_6$, its crystal structure is different from that of $Ba_2LnRuO_6$ and $Sr_2LnRuO_6$ compounds in which both the rare earth ion and the ruthenium ion occupy B sites [2, 4, 6]. For $Ca_2LnRuO_6$, smaller Ln ions should occupy the B site of the perovskite $ABO_3$, while larger Ln ions may replace the Ca ions of the A site. Previously, we prepared a series of $Ca_2LnRuO_6$ compounds (Ln =Y, La–Lu) and studied systematically their crystal structures [15, 16]. The X-ray diffraction measurements showed that for larger Ln ions $Ca^{2+}$ and $Ln^{3+}$ ions were partially disordered at the A site and half of the B site of the perovskite $ABO_3$, and that $Ca^{2+}/Ln^{3+}$ and $Ru^{5+}$ ions located at the B site were regularly ordered. Therefore, these compounds should be represented by $Ca_{2-x}Ln_x[Ln_{1-x}Ca_x]RuO_6$ [16]. The ratio of the $Ln^{3+}$ ion located at the B site varied with its ionic radius. In the $Ca_2LnRuO_6$, the small size of the A site cation results in the large distortion of the perovskite from the cubic symmetry. As a result, the magnetic transition temperatures of $Ca_2LnRuO_6$ were much lower than those of the corresponding $Ba_2LnRuO_6$ and $Sr_2LnRuO_6$, for example 10 K ($Ca_2PrRuO_6$) and 11.5 K ($Ca_2NdRuO_6$) [15].

We focused our attention on the high antiferromagnetic transition temperatures for $Ba_2PrRuO_6$ and $Ba_2NdRuO_6$ [9, 10]. The corresponding strontium compounds $Sr_2PrRuO_6$ and $Sr_2NdRuO_6$ were not prepared [7]. Although $Ca_2PrRuO_6$ and $Ca_2NdRuO_6$ compounds were

formed, they were actually $CaLn[CaRu]O_6$, i.e., the Pr and Nd ions are located not at the B site, but at the A site [16].

In this study, we tried to prepare $SrCa[LnRu]O_6$ type compounds. In such compounds, since the larger Sr ion is situated at the A-site, the distortion of these double perovskites from the cubic symmetry should be smaller than that for the $Ca_2LnRuO_6$ (actually $CaLn[CaRu]O_6$). If the Pr and Nd ions were situated at the B site of the perovskite $ABO_3$, i.e., the $SrCa[PrRu]O_6$ and $SrCa[NdRu]O_6$ were formed, the effect of the A site cations on the magnetic properties of Pr (Nd) and Ru ions will be elucidated by comparing the magnetic properties of $SrCaLnRuO_6$ with those of $Ba_2LnRuO_6$. We performed X-ray diffraction measurements to determine their crystal structures, and measured their magnetic susceptibility and specific heat down to 1.8 K.

## 2. Experimental

Polycrystalline samples of $SrCaLnRuO_6$ were prepared by firing the appropriate amounts of $CaCO_3$, $SrCO_3$, $Ln_2O_3$ (Ln = La, Nd–Gd, Dy–Lu) or $Pr_6O_{11}$, and $RuO_2$, at 1373–1473K for 24 hr with frequent grindings and pelletings. X-ray powder diffraction measurements were performed on a Rigaku RINT 2100 diffractometer. The structure and lattice parameters were refined with a Rietveld program RIETAN 2000 [17]. Magnetic susceptibility measurements were performed under both the zero-field-cooled (ZFC) and field-cooled (FC) conditions with a

SQUID magnetometer (Quantum Design MPMS model). The former was measured on heating the samples to 300 K after zero-field cooling to 1.8 K. The applied magnetic field was 0.1 T. The latter was measured on cooling the samples from 300 to 1.8 K at 0.1 T. The specific heat measurements were carried out using a relaxation technique supplied by the commercial heat capacity measurement system (Quantum Design, Model PPMS). The sample in the form of a pellet (~ 10 mg) was mounted on an alumina plate with apiezon for better thermal contact. The specific heat and magnetic susceptibility were measured in the temperature range from 1.8 to 300 K.

## 3. Results and discussion

### *3.1. Crystal structure*

Measurements of the X-ray diffraction patterns show that Ln = La, Pr, and Nd compounds crystallize as the perovskite phase. For Ln = Sm, Eu, and Gd, Ru-rich perovskite-phases $Sr_3CaRu_2O_9$ were formed [18], in which Ln ions are solid-solved and a small amount of the impurity phase was also observed. For smaller Ln ions, the desired compounds were not obtained. The stable $Ln_2O_3$ did not react well with the other starting materials.

Figure 1 shows the X-ray diffraction profile for $SrCaLaRuO_6$. All the powder X-ray diffraction patterns for the compounds prepared as a monoclinic single phase were indexed with

the space group $P2_1/n$. The total intensity for (0 0 2) and (1 1 0) appeared at $2\theta \sim 22^\circ$ is significantly small, compared with the compounds in which both Ln and Ru ions are occupied completely at the B site. This fact reflects that $Ca^{2+}$ ions partially occupy the B sites. The present case is the same with that for $Ca_2LnRuO_6$ (Ln = La ~ Gd) [16]. In addition, the (0 1 1) and (1 0 1) peaks observed at $2\theta \sim 19^\circ$ indicate the structural cation ordering between B' and B" sites. In order to clarify the exact cation distribution in this $SrCaLnRuO_6$ series, the X-ray diffraction data were analyzed by the Rietveld method with using RIETAN 2000 program [17]. The results of this analysis show that $Ca^{2+}$ ions partially occupy the B site, i.e. the $SrCaLnRuO_6$ is represented as $SrCa_{1-x}Ln_x[Ln_{1-x}Ca_x]RuO_6$. In addition, they show that the B' and B" ions are regularly ordered in the NaCl-type. The B" site is occupied by only the $Ru^{5+}$ ion and the B' site is randomly occupied by $Ca^{2+}$ and $Ln^{3+}$ ions. Figure 2 shows the schematic crystal structure for $SrCaLnRuO_6$, and the structural parameters determined for $SrCaNdRuO_6$ are listed in Table 1.

Figure 3 shows the variation of the occupancy $x$ (the ratio of the $Ca^{2+}$ ions at the B' site) with the $Ln^{3+}$ ionic radius. It is revealed that the $x$ value depends on the $Ln^{3+}$ radius. For the compounds with Ln = La, the $Ca^{2+}$ ion mainly occupies the B' site (x ~ 0.93). From Ln =Pr to Nd, the ratio of the $Ca^{2+}$ ion at the B' site is gradually decreased. The cation disorder of the B' and A sites found in this $SrCaLnRuO_6$ series is also due to the fact that the ionic radius of $Ca^{2+}$ (1.00 Å) is near to that of $Ln^{3+}$. In the same figure, the x values for $Ca_2LnRuO_6$ compounds

were also shown. It is clear that the x values for $SrCaLnRuO_6$ are smaller than those for $Ca_2LnRuO_6$, which is due to the fact that larger Sr ions stably occupy the A site and increase the average ionic radius of the A-site cations.

The lattice parameters and reliability factors for $SrCaLnRuO_6$ (Ln = La, Pr, Nd) are listed in Table 2. The lattice parameters *a*, *b* and *c* tend to decrease with decreasing the $Ln^{3+}$ ionic radius. The values of $\beta$ increase with decreasing the $Ln^{3+}$ ionic radius, indicating that these double perovskites (actually $[SrLn][CaRu]O_6$) distort greatly from the cubic symmetry, because of its smaller difference in the ionic radius between A-site and B-site cations.

*3.2. Magnetic properties of $SrCaLaRuO_6$*

The magnetic susceptibilities of $SrCaLaRuO_6$ are plotted as a function of temperature in Fig. 4. It is found that an antiferromagnetic transition occurs at $T_N$ =10 K. The magnetic properties of $SrCaLaRuO_6$ are due to the $Ru^{5+}$ ion because $La^{3+}$ ion is diamagnetic. Its reciprocal magnetic susceptibility versus temperature curve (the inset of Fig. 4) was fitted with the Curie–Weiss law in the temperature range between 100 and 300 K. The effective magnetic moment and Weiss constant were obtained to be 3.89 $\mu_B$ and -134 K, respectively. The effective magnetic moment is close to the spin-only value for the $Ru^{5+}$ ion with $S$ = 3/2 (3.87 $\mu_B$). The large negative Weiss constant indicates the antiferromagnetic interaction between $Ru^{5+}$ ions.

The large divergence between the ZFC and FC susceptibilities has been found. This result indicates that $SrCaLaRuO_6$ is not an ideal antiferromagnet. This should be due to the contribution of the weak ferromagnetic component to the magnetic properties. In the case of the compound with low crystal symmetry such as monoclinic symmetry, the Dzyaloshinsky-Moriya (D-M) interaction can exist between the ordered moments, which results in the existence of a weak ferromagnetic component in its magnetic susceptibilities.

Figure 5 (a) shows the temperature dependence of the specific heat $C_p$ for $SrCaLaRuO_6$. The specific heat data also show a λ-type anomaly at the same temperature, 10 K. To calculate the magnetic contribution to the specific heat, we have to subtract the contribution of lattice specific heat from the total specific heat. They were estimated by using a polynomial function of the temperature, $f(T) = aT^3 + bT^5 + cT^7$ [19], in which the constants $a$, $b$ and $c$ were determined by fitting this function to the observed specific heat data above 30 K. Figure 5 (b) shows the temperature dependence of the magnetic specific heat divided by temperature ($C_{mag}/T$). From the temperature dependence of the magnetic specific heat, the magnetic entropy change of $SrCaLaRuO_6$ is calculated by the relation $S_{mag} = \int (C_{mag}/T) dT$. It is also shown in Fig. 5 (b). The magnetic entropy change due to the antiferromagnetic ordering of $Ru^{5+}$ ions in the $SrCaLaRuO_6$ is about 4.8 J $mol^{-1}$ $K^{-1}$.

In an octahedral crystal field environment, the ground state of the $Ru^{5+}$ ion ($4d^3$, the state

$^4F_{3/2}$) is the four-fold degenerate state. The magnetic entropy change of $Ru^{5+}$ is calculated to be $R\ln(2S+1) = 11.5$ Jmol$^{-1}$ K$^{-1}$, where $R$ and $S$ are the molar gas constant and the spin quantum number, respectively. In the case of lower symmetry, this state splits into two Kramers doublet states. For such a case, the magnetic entropy change is expected to be $R\ln 2 = 5.76$ J mol$^{-1}$ K$^{-1}$. The result of the magnetic entropy change indicates that the degeneracy of the ground state for the $Ru^{5+}$ ion in $SrCaLaRuO_6$ should be doublet. These results for $SrCaLaRuO_6$ are quite similar to those for $Ca_2LaRuO_6$ (more precisely, $[CaLa][CaRu]O_6$), which means that the difference in the crystal structure between $SrCaLaRuO_6$ and $Ca_2LaRuO_6$ is negligible in their magnetic properties. This result is plausible, because the magnetic ion at the B-site is only the $Ru^{5+}$ ion for both the $SrCaLaRuO_6$ and $Ca_2LaRuO_6$.

*3.3. Magnetic properties of $SrCaPrRuO_6$*

The magnetic susceptibility for $SrCaPrRuO_6$ is plotted as a function of temperature in Fig. 6. This compound shows an antiferromagnetic transition at 12 K. Compared with the antiferromagnetic transition temperature for $SrCaLaRuO_6$, the transition temperature for $SrCaPrRuO_6$ increased, which may reflect the contribution of paramagnetic $Pr^{3+}$ to the antiferromagnetic interaction. Another anomaly in the ZFC magnetic susceptibility was found at 5 K.

In the inset of Fig. 6, the reciprocal susceptibility was plotted against temperature. The fitting of the Curie-Weiss law gives 5.07 $\mu_B$ and -69 K, respectively. Since the theoretical magnetic moments of $Ru^{5+}$ and $Pr^{3+}$ are 3.87 and 3.58 $\mu_B$, respectively, the expected effective magnetic moment (5.27$\mu_B$) is estimated from the relation $\mu_{\text{eff}} = \sqrt{\mu_{Ru^{5+}}{}^2 + \mu_{Pr^{3+}}{}^2}$. The value obtained from the experiment is a little lower than the calculated value. This result may suggest that the magnetic ions in this compound are affected by the crystal field to some extent. The negative Weiss constant indicates that the predominant magnetic interaction in $SrCaPrRuO_6$ is antiferromagnetic.

*3.4. Magnetic properties of $SrCaNdRuO_6$*

Figure 7 shows the temperature dependence of the magnetic susceptibility for $SrCaNdRuO_6$. This compound also shows an antiferromagnetic transition at 12 K. Below this temperature, the ZFC and FC susceptibilities diverged. Another anomaly in the ZFC susceptibility is observed at ca. 2 K. These results are quite similar to those for $SrCaPrRuO_6$. The magnetic susceptibility obeys the Curie–Weiss law in the temperature range between 80 and 300 K. The effective magnetic moment and Weiss constant were obtained to be 5.15 $\mu_B$ and -76 K, respectively. Since the theoretical magnetic moments of $Ru^{5+}$ and $Nd^{3+}$ are 3.87 and 3.62 $\mu_B$, respectively, the effective magnetic moment for $SrCaNdRuO_6$ is calculated to be 5.30$\mu_B$.

The experimental value is close to the moment estimated from this calculation.

In order to clarify the two magnetic anomalies at low temperatures, specific heat measurements were performed down to 1.8 K. The temperature dependence of the specific heat for $SrCaNdRuO_6$ is shown in Fig. 8 (a). Figure 8 (b) shows the dependence of the magnetic specific heat divided by temperature ($C_{mag}/T$) below 40 K. The magnetic specific heat ($C_{mag}$) is obtained from the specific heat data in the same way as is the case for $SrCaLaRuO_6$. It is found that both the $C_p$ vs. $T$ and $C_{mag}/T$ vs. $T$ curves show two anomalies at 12 and 5 K. The anomaly at 12 K seems to correspond to the antiferromagnetic behavior found in the magnetic susceptibility measurements. Comparing the fact that the $SrCaLaRuO_6$ shows an antiferromagnetic transition at 10 K, the magnetic behavior observed for $SrCaNdRuO_6$ at 12 K is also due to magnetic interactions between $Ru^{5+}$ ions. The higher magnetic transition temperature for $SrCaNdRuO_6$ than that for $SrCaLaRuO_6$ should be due to the contribution of paramagnetic $Nd^{3+}$ ion to this antiferromagnetic interaction.

For the specific heat anomaly at 5 K, the corresponding anomaly is not observed in the magnetic susceptibility measurements. As shown in Fig. 7, both the ZFC and FC susceptibilities still increased with decreasing temperature, and below 2.0 K, the ZFC susceptibility began to decrease with decreasing temperature. Namely, the $Nd^{3+}$ ion is still in the paramagnetic state at 5 K. We consider that the observed anomaly in the specific heat is due to not the magnetic

ordering, but the Schottky-type anomaly of the $Nd^{3+}$ ion, as is the case for $Ca_2NdRuO_6$ [15].

Figure 8 (b) also shows the temperature dependence of the magnetic entropy change for $SrCaNdRuO_6$. The total magnetic entropy change due to these two anomalies is approximately 8.3 J $mol^{-1}$ $K^{-1}$. Owing to the difficulty in dividing the magnetic entropy data into two anomalies, we cannot determine the individual $\Delta S_{mag}$ values. Since the magnetic entropy change due to the antiferromagnetic ordering of $Ru^{5+}$ ions in the $SrCaLaRuO_6$ is experimentally obtained to be 4.8 J $mol^{-1}$ $K^{-1}$, the rest of the magnetic entropy change is estimated to be 3.5 J $mol^{-1}$ $K^{-1}$. The ground multiplet $^4I_{9/2}$ of $Nd^{3+}$ ion splits into five Kramers' doublets in a crystal field with low symmetry. The ground doublet is selectively populated at low temperatures, and the magnetic entropy is expected to be $R$ ln2 = 5.76 J $mol^{-1}$ $K^{-1}$. Although the estimated value (3.5 J $mol^{-1}$ $K^{-1}$) is smaller than the value 5.76 J $mol^{-1}$ $K^{-1}$, this result indicates that the ground state of the $Nd^{3+}$ ion should be a Kramers' doublet. The reason for the smaller magnetic entropy change obtained experimentally is that we do not include the magnetic entropy change at very low temperatures due to still offset of the magnetic ordering of $Nd^{3+}$ ions.

## 4. Summary

X-ray diffraction measurements on $SrCaLnRuO_6$ (Ln = La, Pr, Nd) show that $Ca^{2+}$ and $Ln^{3+}$ ions are partially disordered at the A site and half of the B site of the perovskite $ABO_3$, and

that $Ca^{2+}/Ln^{3+}$ and $Ru^{5+}$ ions are regularly ordered at the B site. These compounds order antiferromagnetically at 10 – 12 K, due to the magnetic interactions between $Ru^{5+}$ ions.

**Acknowledgements**

This work was supported by Grant-in-aid for Scientific Research of Priority Area "Panoscopic Assembling and High Orderd Functions for Rare Earth Materials" No. 20900103 and Grant-in-aid for Scientific Research, No. 20550052 from the Ministry of Education, Science, Sports, and Culture of Japan.

**References**

[1] M. T. Anderson, K. B. Greenwood, G. A. Taylor, and K. R. Poeppelmeier, Proc. Solid State Chem., **22** (1993) 197-233.

[2] P.D. Battle, J.B. Goodenough, and R. Price, J. Solid State Chem., **46** (1983) 234-244.

[3] P.D. Battle and W.J. Macklin, J. Solid State Chem., **52** (1984) 138-145.

[4] P.D. Battle and W.J. Macklin, J. Solid State Chem., **54** (1984) 245-250.

[5] P.D. Battle and C.W. Jones, J. Solid State Chem., **78** (1989) 108-116.

[6] P.D. Battle, C.W. Jones, and F. Studer, J. Solid State Chem., **90** (1991) 302-312.

[7] Y. Doi and Y. Hinatsu, J. Phys.: Condens. Matter, **11** (1999) 4813-4820.

[8] Y. Doi, Y. Hinatsu, K. Oikawa, Y. Shimojo, and Y. Morii, J. Mater. Chem., **10** (2000) 797-800.

[9] Y. Izumiyama, Y. Doi, M. Wakeshima, Y. Hinatsu, K. Oikawa, Y. Shimojo, and Y. Morii, J. Mater. Chem., **10** (2000) 2364-2367.

[10] Y. Izumiyama, Y. Doi, M. Wakeshima, Y. Hinatsu, Y. Shimojo, and Y. Morii, J. Phys.: Condens. Matter, **13** (2001) 1303-1313.

[11] Y. Izumiyama, Y. Doi, M. Wakeshima, Y. Hinatsu, A. Nakamura, and Y. Ishii, J. Solid State Chem. **169** (2002) 125-130.

[12] Y. Hinatsu and Y. Doi, Bull. Chem. Soc. Japan, **76** (2003) 1093-1113.

[13] N. G. Parkinson, P. D. Hatton, J. A. K. Howard, C. Ritter, R. M. Ibberson, and M-K Wu, Y. Izumiyama, Y. Doi, M. Wakeshima, Y. Hinatsu, Y. Shimojo, and Y. Morii, J. Phys.: Condens. Matter, **16** (2004) 7611-7624.

[14] R. Saez-Puche, E. Climent-Pascual, R. Ruiz-Bustos, M. A. Alario-Franco, and M. T. Fernandez-Diaz, Progress in Solid State Chem., **35** (2007) 211-219.

[15] C. Sakai, Y. Doi, Y. Hinatsu, and K. Ohoyama, J. Phys.: Condens. Matter, **17** (2005) 7383-7394.

[16] C. Sakai, Y. Doi, and Y. Hinatsu, J. Alloys and Compounds, **408-412** (2006) 608-612.

[17] F. Izumi and T. Ikeda, Mater. Sci. Forum, **198** (2000) 321–324.

[18] J. T. Rijssenbeek, S Malo, V. Caignaert, and K. R. Poeppelmeier, J. Amer. Chem. Soc., **124** (2002) 2090-2091.

[19] J.E. Gordon, R.A. Fisher, Y.X. Jia, N.E. Phillips, S.F. Reklis, D.A. Wright, and A. Zettl, Phys. Rev., B **59** (1999) 127-130.

## FIGURE CAPTIONS

Fig.1 Powder x-ray diffraction profiles for $SrCaLaRuO_6$. The calculated and observed profiles are shown on the top solid line and cross markers, respectively. The vertical marks in the middle show positions calculated for Bragg reflections. The lower trace is a plot of the difference between calculated and observed intensities.

Fig.2 The schematic crystal structure for $SrCaLnRuO_6$ (Ln = La, Pr, Nd).

Fig.3 The ratio of the $Ca^{2+}$ ions at the B' site of the double perovskite $A_2B'RuO_6$. For comparison, the data for $Ca_2LnRuO_6$ were also shown.

Fig.4 Temperature dependence of the magnetic susceptibility for $SrCaLaRuO_6$. The inset shows the reciprocal susceptibility vs. temperature curve. The solid line is the Curie-Weiss fitting.

Fig.5 (a) Temperature dependence of the specific heat $C_p$ for $SrCaLaRuO_6$. The inset shows the detailed temperature dependence below 40 K. The solid line is the calculation results for the lattice specific heat (see text). (b) Temperature dependences of the magnetic specific heat divided by temperature $C_{mag}/T$ and the magnetic entropy change $S_{mag}$ for $SrCaLaRuO_6$ below 40 K.

Fig.6 Temperature dependence of the magnetic susceptibility for $SrCaPrRuO_6$. The inset shows the reciprocal susceptibility vs. temperature curve. The solid line is the

Curie-Weiss fitting.

Fig.7 Temperature dependence of the magnetic susceptibility for $SrCaNdRuO_6$. The inset shows the detailed temperature dependence below 40 K.

Fig.8 (a) Temperature dependence of the specific heat $C_p$ for $SrCaNdRuO_6$. The inset shows the detailed temperature dependence below 40 K. The solid line is the calculation results for the lattice specific heat (see text). (b) Temperature dependences of the magnetic specific heat divided by temperature $C_{mag}/T$ and the magnetic entropy change $S_{mag}$ for $SrCaNdRuO_6$ below 40 K.

Table 1 Atomic positional parameters for $SrCaNdRuO_6$

| Atom | site | occupancy | x | y | z | $B$ (Å$^2$)* |
|---|---|---|---|---|---|---|
| Sr1 | 4e | 0.5 | 0.5197(5) | 0.550(3) | 0.253(6) | 0.55 |
| Ca1 | 4e | 0.085(4) | 0.5197(5) | 0.550(3) | 0.253 (6) | 0.55 |
| La1 | 4e | 0.415(4) | 0.5197(5) | 0.550(3) | 0.253 (6) | 0.55 |
| Ru1 | 2d | 1.0 | 1/2 | 0 | 0 | 0.22 |
| Ca2 | 2c | 0.830(7) | 0 | 1/2 | 0 | 0.43 |
| La2 | 2c | 0.170(7) | 0 | 1/2 | 0 | 0.43 |
| O1 | 4e | 1.0 | 0.205(3) | 0.229(4) | −0.023 (4) | 1.08 |
| O2 | 4e | 1.0 | 0.318(3) | 0.718(4) | −0.070(3) | 1.08 |
| O3 | 4e | 1.0 | 0.384(3) | −0.036(3) | 0.211 (3) | 1.08 |

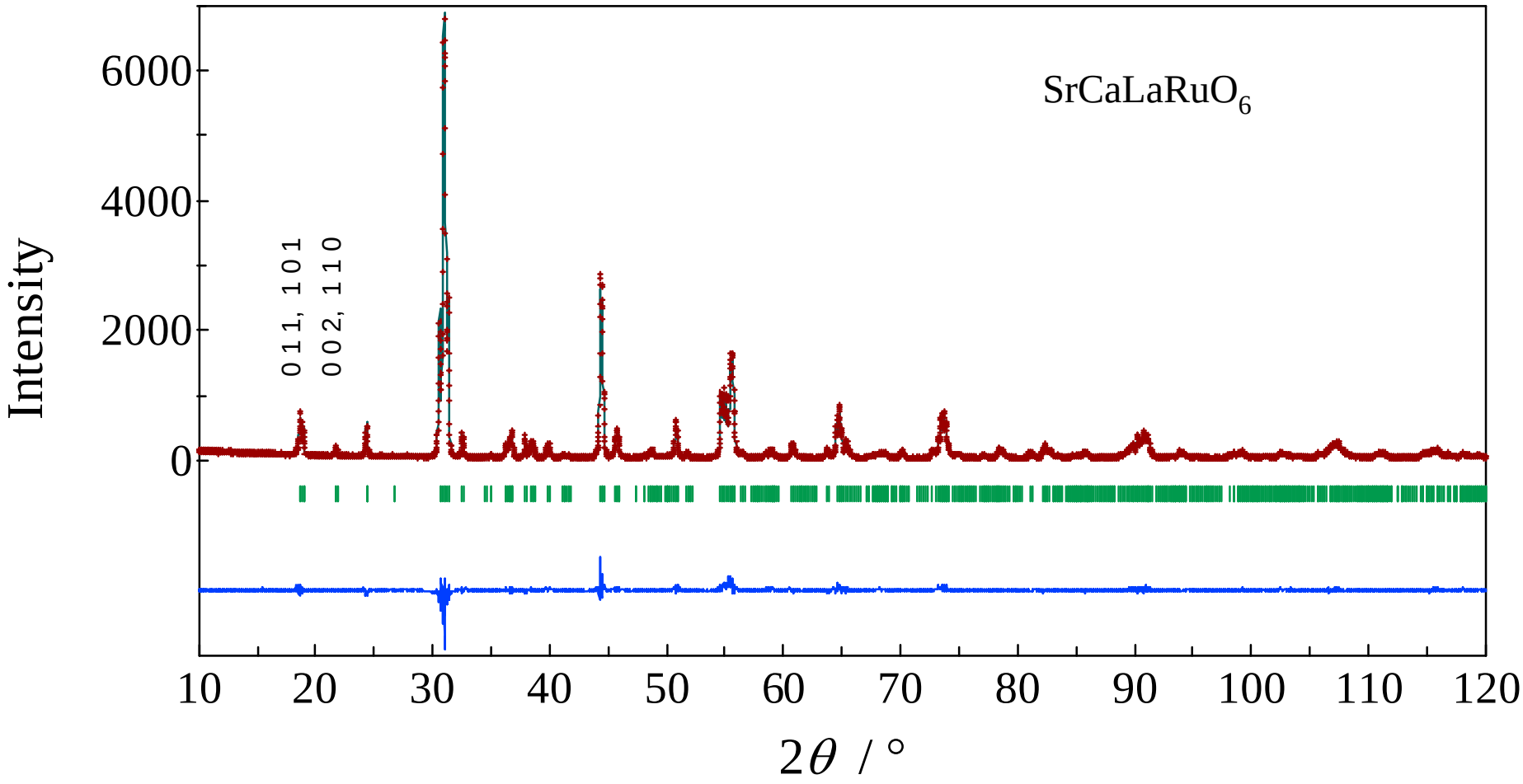
* The values for B are fixed to the values for $Ca_2LaRuO_6$ [16].

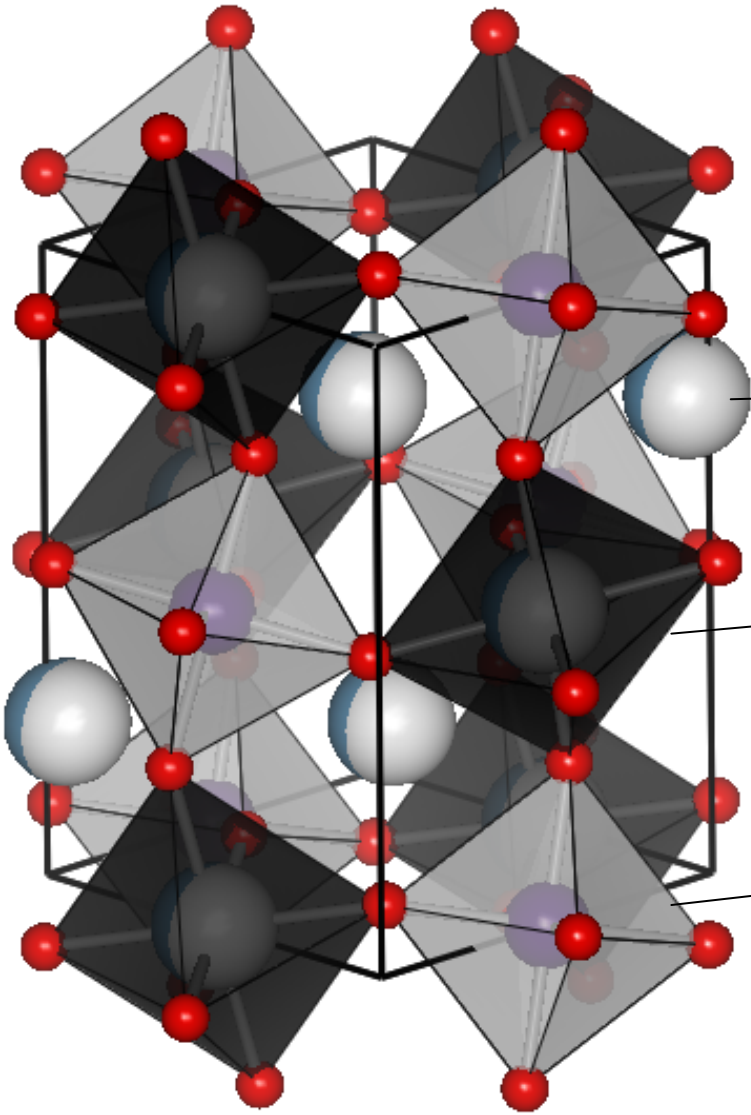
Table 2 Lattice parameters and reliability factors for SrCa*Ln*$RuO_6$

| *Ln* | a/ Å | b/ Å | c/ Å | β/° | *V*/ Å$^3$ | $R_{wp}$/% | $R_I$/% |
|---|---|---|---|---|---|---|---|
| La | 5.7187(3) | 5.8498(3) | 8.1562(4) | 90.241(2) | 272.85(2) | 11.67 | 5.43 |
| Pr | 5.6714(3) | 5.8475(3) | 8.1090(5) | 90.268(2) | 268.92(3) | 11.09 | 3.89 |
| Nd | 5.6716(9) | 5.8450(9) | 8.0979(11) | 90.2724(6) | 268.45(7) | 14.82 | 3.54 |

Note. Definition of reliability factors $R_{wp}$ and $R_I$ are given as follows:

$$R_{WP} = \left[\sum w\left(\left|F(o)\right| - \left|F(c)\right|\right)^2 / \sum w\left|F(o)\right|^2\right]^{\frac{1}{2}} \text{ and } R_I = \sum\left|I_k(o) - I_k(c)\right| / \sum I_k(o) .$$

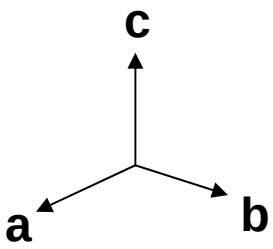

SrCaLaRuO6
Intensity
6000
4000
2000
0
011, 101
002, 110
10
20
30
40
50
60
70
80
90
100
110
120
2θ / °

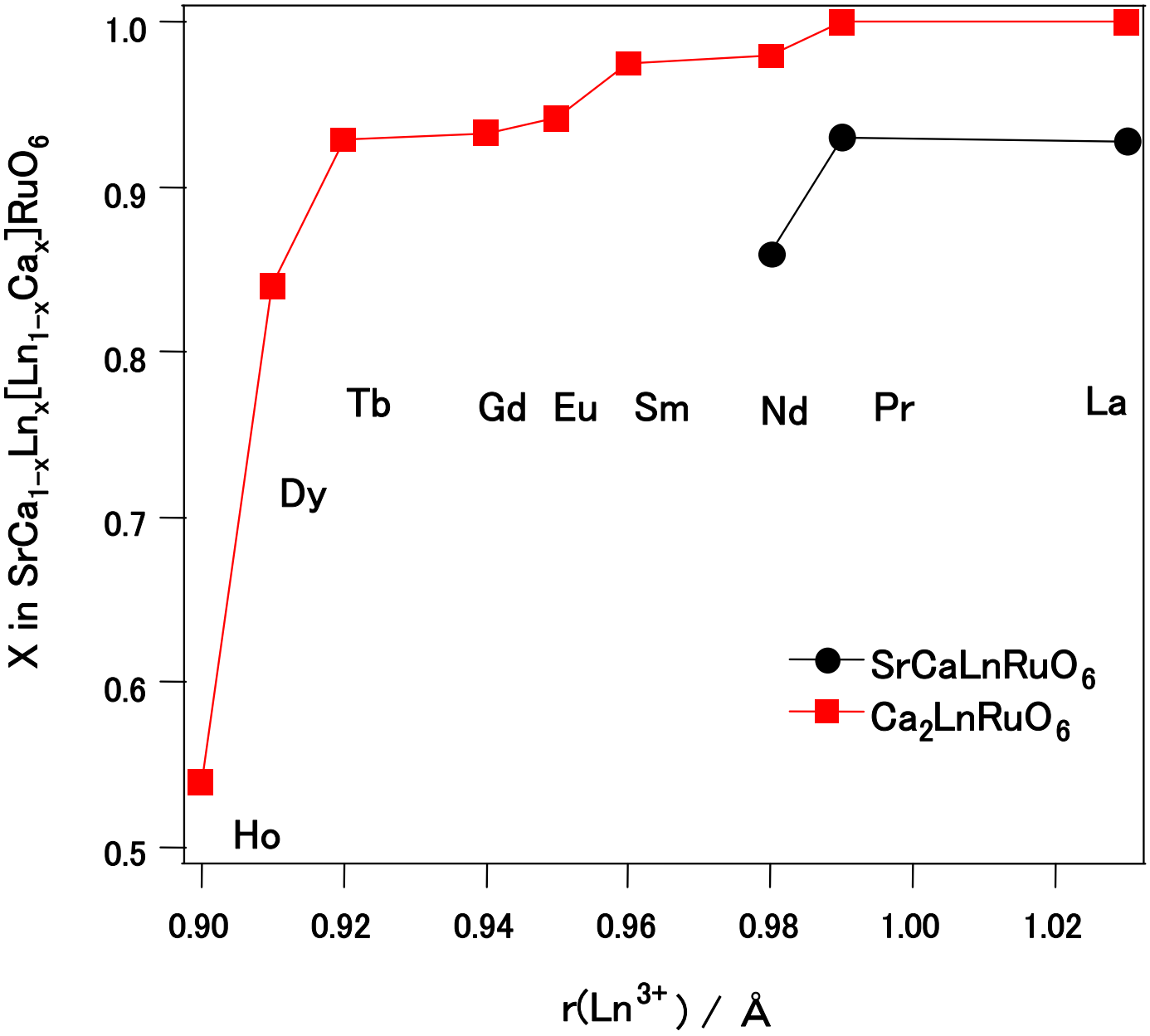


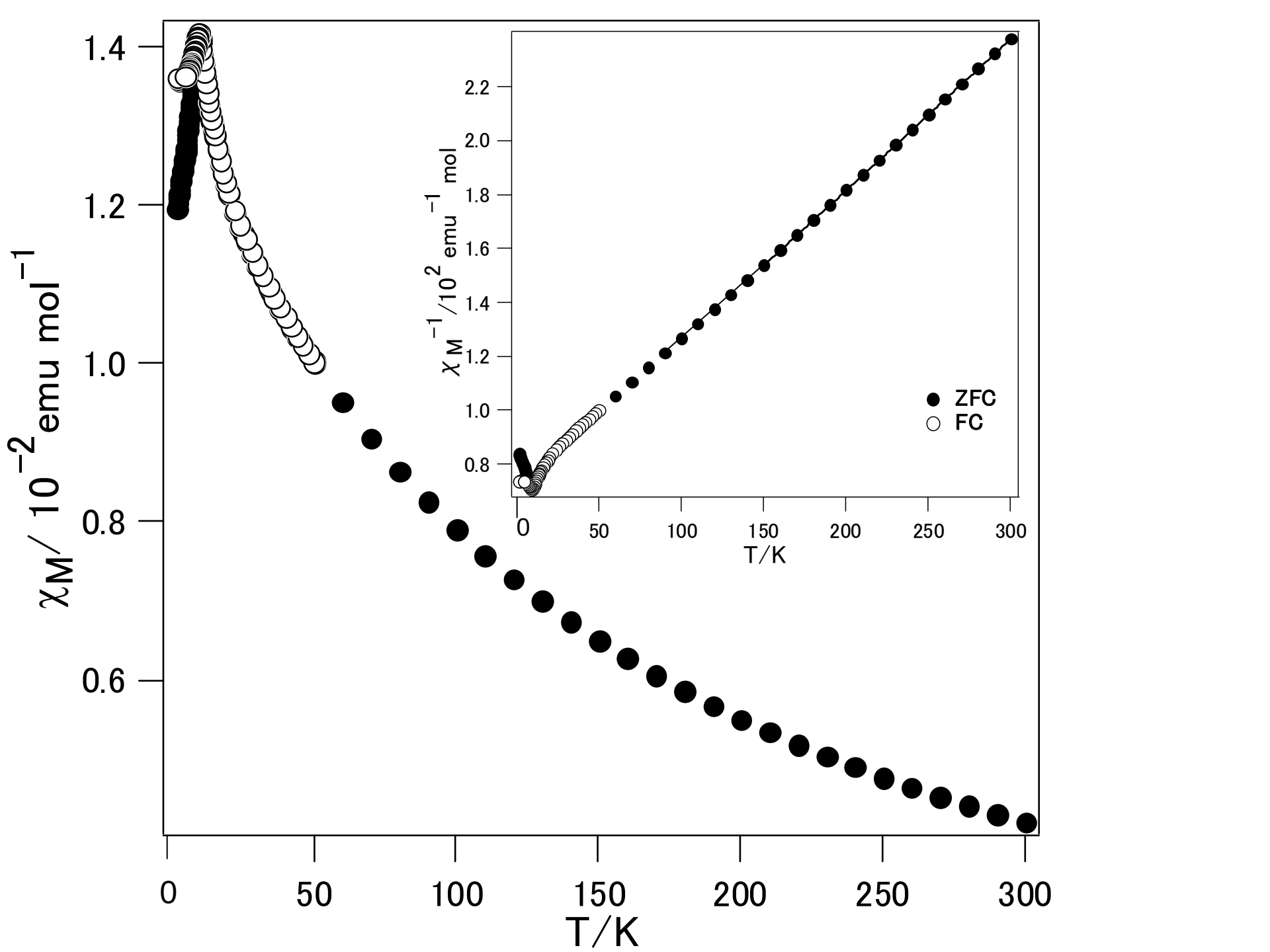
A (A = Sr or $Ca_{1-x}Ln_x$)

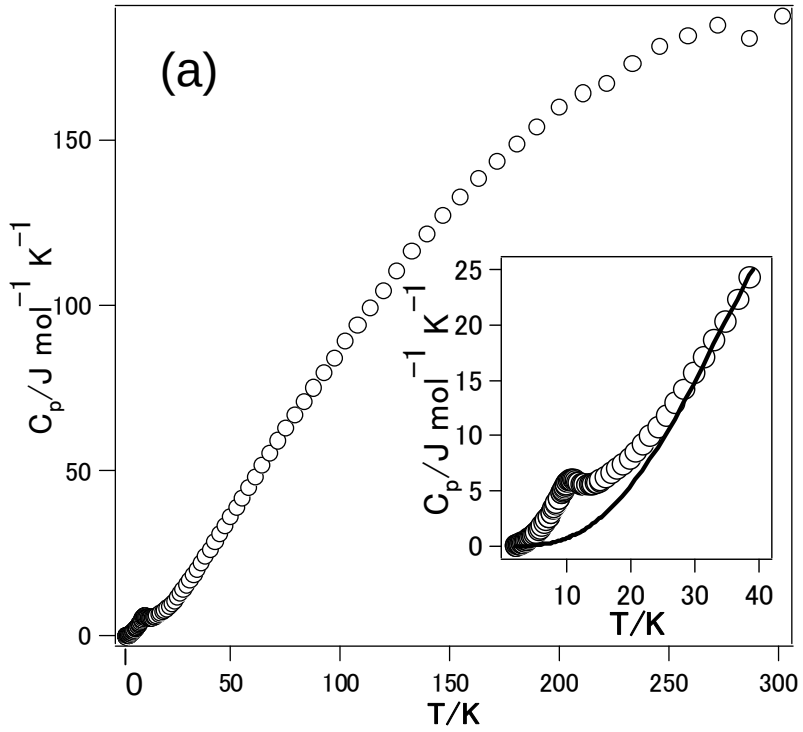
$B'O_6$ ($B = Ca_xLn_{1-x}$)

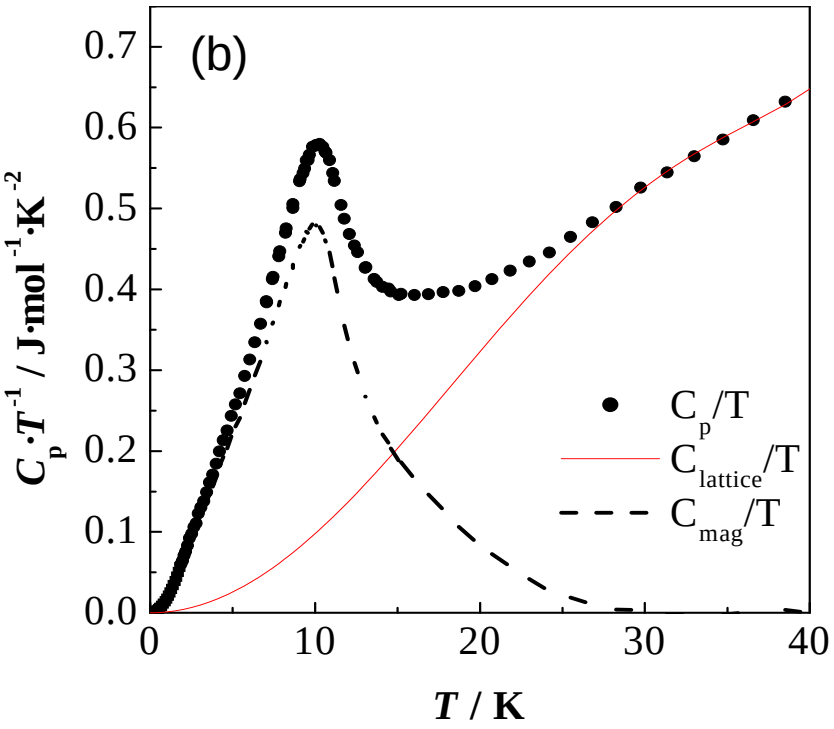
$RuO_6$

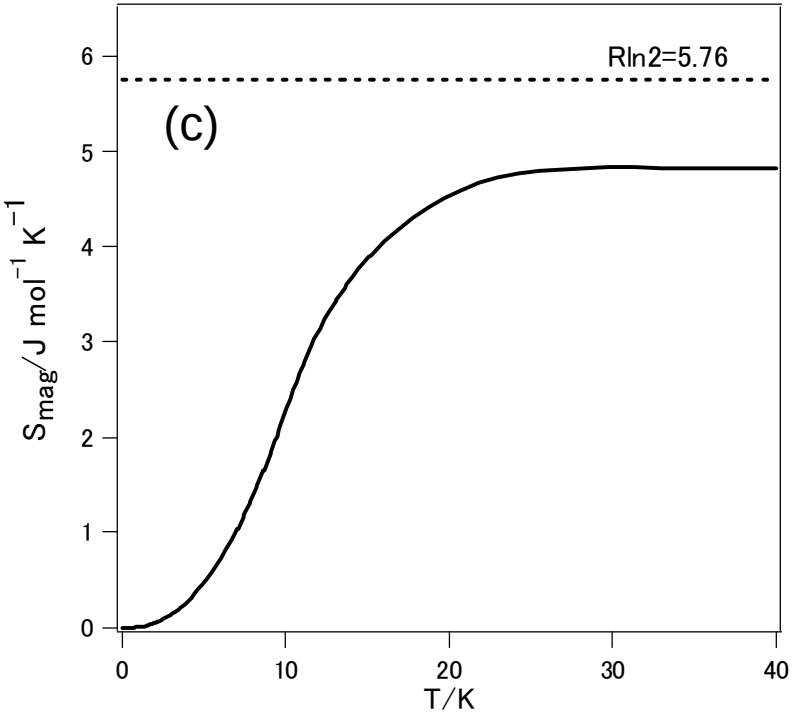


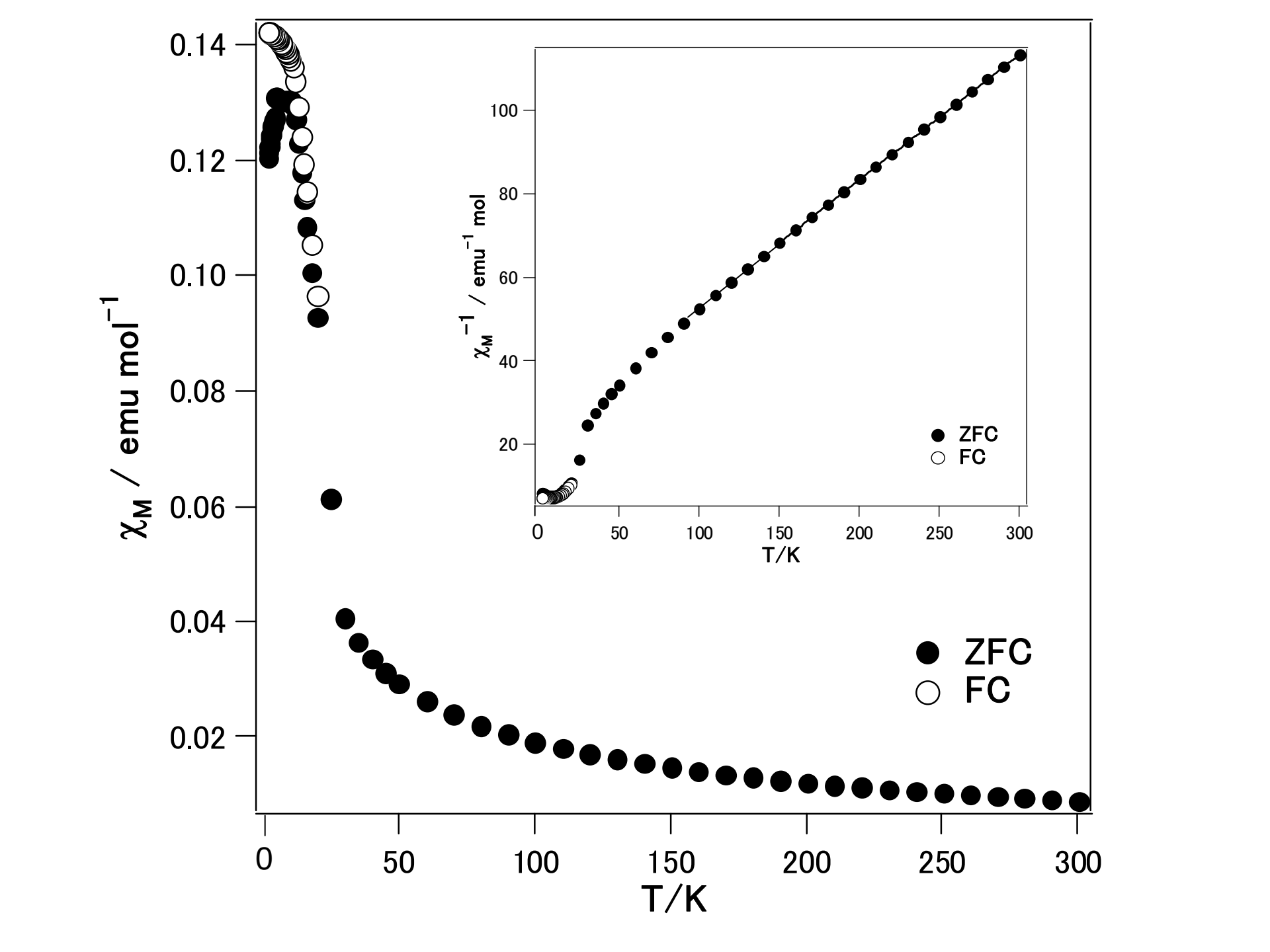

X in SrCa1−xLnx[Ln1−xCax]RuO6
1.0
0.9
0.8
0.7
0.6
0.5
Ho
Dy
Tb
Gd
Eu
Sm
Nd
Pr
La
SrCaLnRuO6
Ca2LnRuO6
0.90
0.92
0.94
0.96
0.98
1.00
1.02
r(Ln3+) / Å

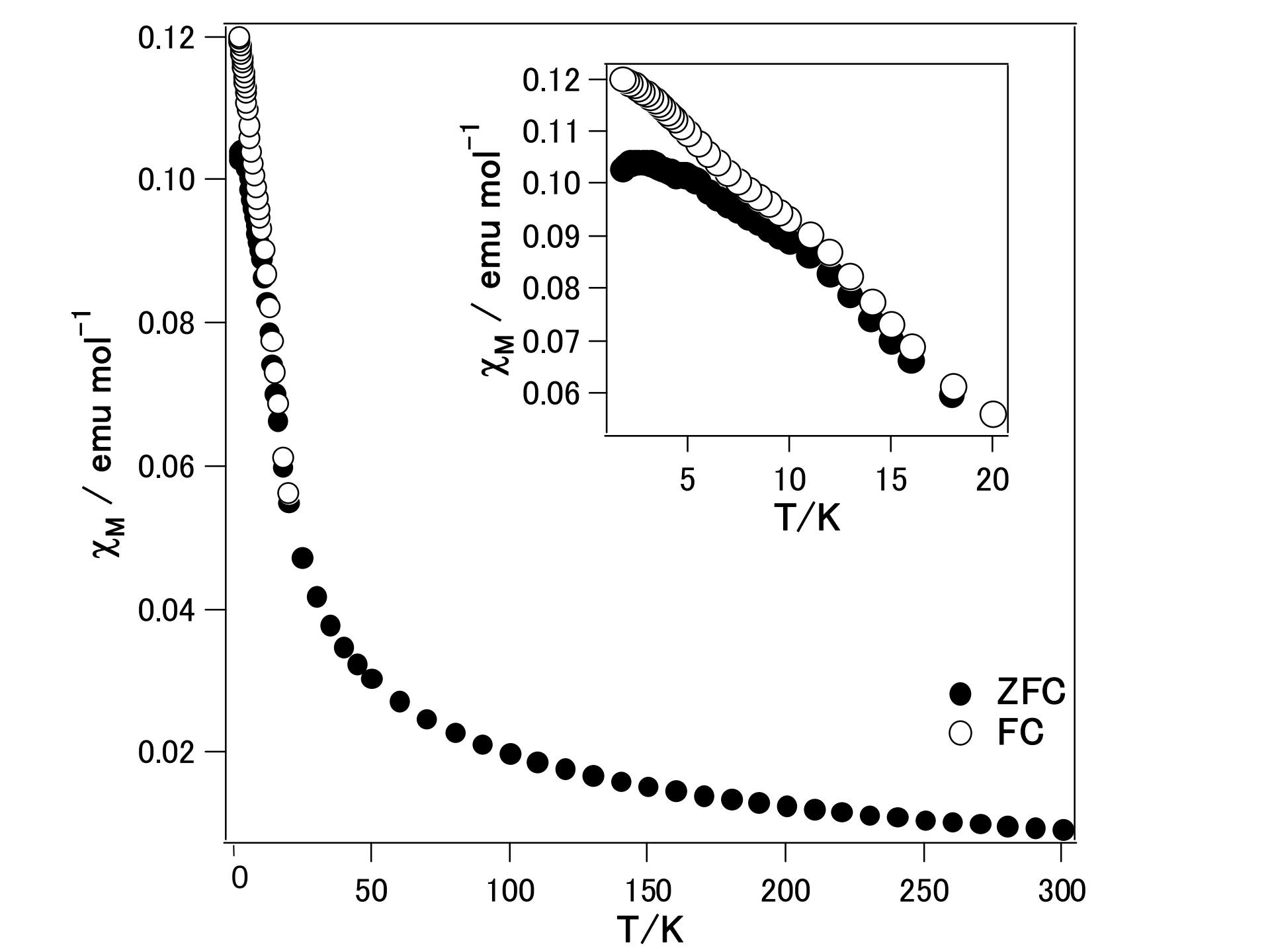

1.4
1.2
1.0
0.8
0.6
$\chi_M$/ $10^{-2}$emu $mol^{-1}$
0
50
100
150
200
250
300
T/K
2.2
2.0
1.8
1.6
1.4
1.2
1.0
0.8
$\chi_M^{-1}$/$10^2$ $emu^{-1}$ mol
ZFC
FC
0
50
100
150
200
250
300
T/K

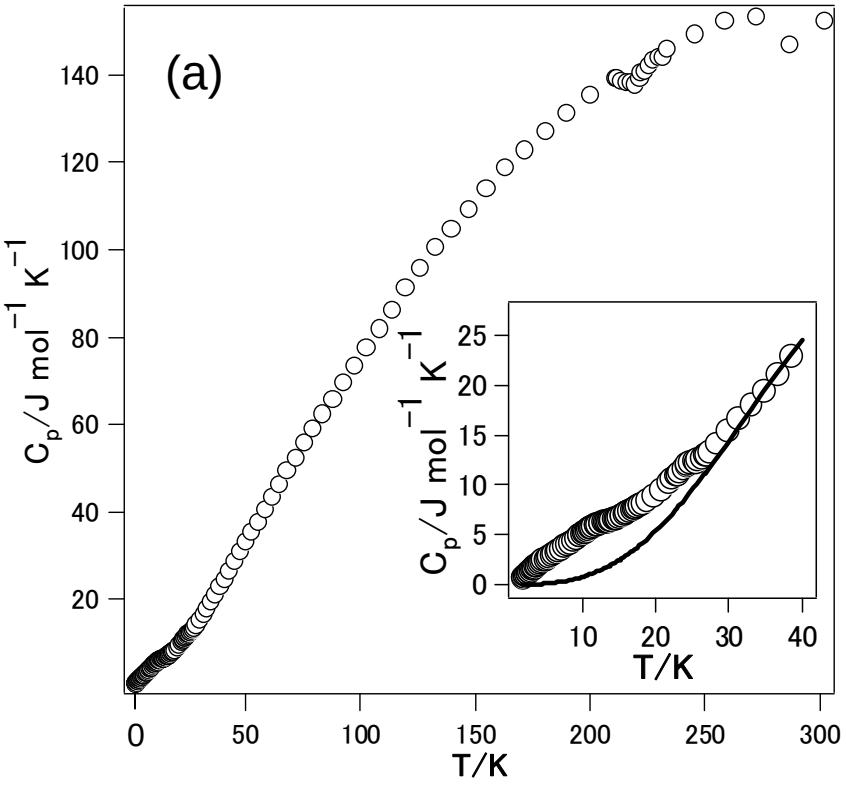

(a)
$C_p$/J mol$^{-1}$ K$^{-1}$
T/K
0
50
100
150
200
250
300
0
50
100
150
$C_p$/J mol$^{-1}$ K$^{-1}$
0
5
10
15
20
25
10
20
30
40
T/K

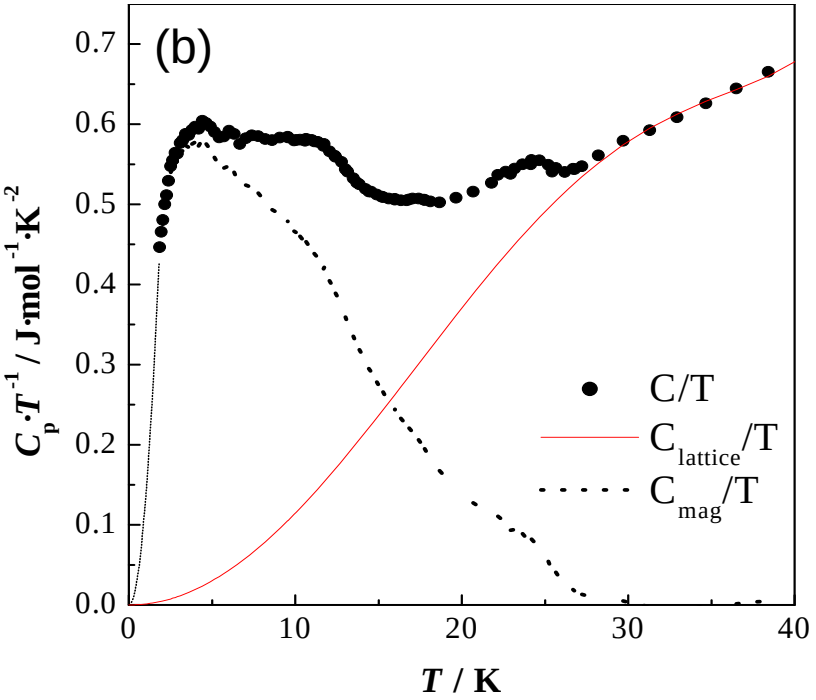

(b)
$C_p \cdot T^{-1}$ / J·mol$^{-1}$·K$^{-2}$
0.0
0.1
0.2
0.3
0.4
0.5
0.6
0.7
0
10
20
30
40
$T$ / K
$C_p$/T
$C_{lattice}$/T
$C_{mag}$/T

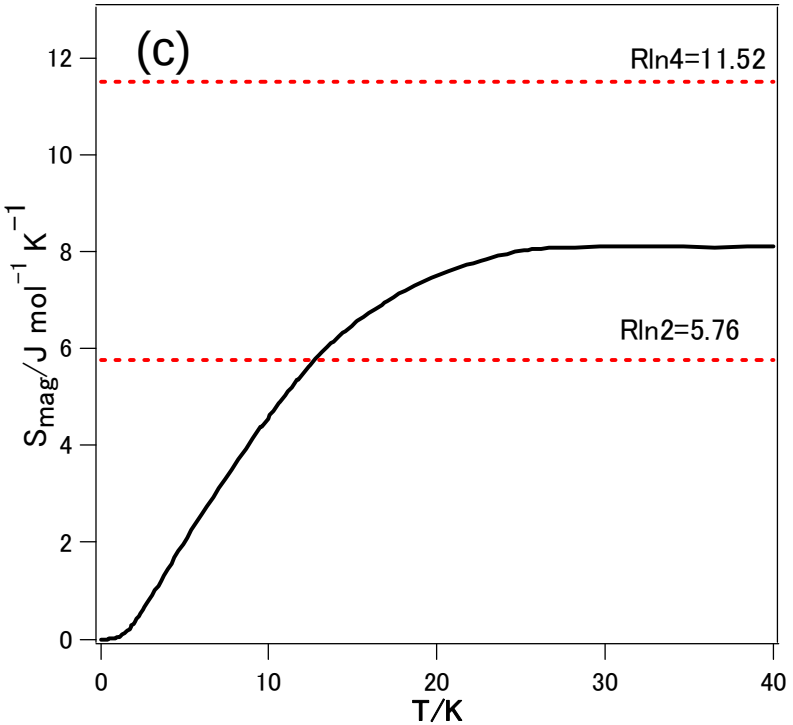

(c)
Rln2=5.76
$S_{mag}$/J mol$^{-1}$ K$^{-1}$
0
1
2
3
4
5
6
0
10
20
30
40
T/K


0.14
0.12
0.10
0.08
0.06
0.04
0.02
χM / emu mol−1
0
50
100
150
200
250
300
T/K
ZFC
FC
100
80
60
40
20
χM−1 / emu−1 mol
0
50
100
150
200
250
300
T/K
ZFC
FC


0.12
0.10
0.08
0.06
0.04
0.02
χM / emu mol−1
0
50
100
150
200
250
300
T/K
ZFC
FC
0.12
0.11
0.10
0.09
0.08
0.07
0.06
χM / emu mol−1
5
10
15
20
T/K


(a)
$C_p$/J mol$^{-1}$ K$^{-1}$
T/K
0
50
100
150
200
250
300
20
40
60
80
100
120
140
$C_p$/J mol$^{-1}$ K$^{-1}$
T/K
0
5
10
15
20
25
10
20
30
40


(b)
$C_p \cdot T^{-1}$ / J·mol$^{-1}$·K$^{-2}$
$T$ / K
C/T
$C_{lattice}$/T
$C_{mag}$/T
0.0
0.1
0.2
0.3
0.4
0.5
0.6
0.7
0
10
20
30
40


(c)
Rln4=11.52
Rln2=5.76
$S_{mag}$/J mol$^{-1}$ K$^{-1}$
T/K
0
2
4
6
8
10
12
0
10
20
30
40